JOURNAL OF CATALYSIS 7, 76–84 (1967)

The Catalytic Decomposition of Nitrous Oxide on Single Crystals of Cobalt Oxide and Cobalt Magnesium Oxide*

MILTON L. VOLPE AND JOHN F. REDDY

From the Argonne National Laboratory, Argonne, Illinois

Received June 11, 1965; revised September 6, 1966

Rate studies have been made of the catalytic decomposition of N_2O on single crystals of CoO with the aim of determining the effect of crystal orientation. In addition, a comparison was made between the activity of CoO {100} and the solid solution (0.60 Co, 0.40 Mg)O {100} to determine the effect of cation dilution. Catalyst outgassing was done in an ultra-high vacuum, reaction temperatures were 500–250°C, and N_2O pressures were usually about 90 torr. Catalyst areas were about 2–5 cm². Although complications were present due to variable effects of pretreatment of the catalysts, the activation energies and pre-exponential factors were found to vary in the order: $\{100\} \cong \{111\} < \{110\}$, in agreement with an elementary application of crystal-field theory to this reaction. In addition, the CoO–MgO catalyst was found to have a lower activity than the pure CoO, and an activation energy that was much higher (39 kcal/mole) for a chemically polished surface than for a mechanically polished one (26 kcal/mole).

INTRODUCTION

The past decade has seen a growth of interest in the structural aspects of heterogeneous catalysis (*1–4*) and much recent research has involved kinetic studies of low surface area catalysts such as thin films (*5*) and single crystals (*6, 7, 8*) rather than the classical high surface area powdered catalysts. The value of single crystals in investigations of the effect of surface structure on catalysis lies in the possibility of characterizing more precisely than in powders the structure of their surfaces. For example, in the present research single crystals were cut along certain chosen crystallographic planes, so that the catalytic activity of those planes alone could be measured.

The heterogeneous decomposition of N_2O, for which *p*-type semiconducting oxides such as CoO and NiO are excellent catalysts (*9–12*) has been studied extensively in the past with conventional powder techniques. Most of this work has been concerned with relating the activity of these oxides in the N_2O decomposition to their semiconducting properties (*13–16*); very little has been done on the possible effect of their surface structure. On the basis that the rate-determining step is an adsorption or desorption (*12, 15, 17*) it would be expected that different crystal faces of these semiconductors would exhibit different catalytic activities. If such a process involves an electron transfer (*9, 10, 12, 15*), the activities would be expected to be effected by the Fermi level or by the value of the electronic work function of the catalysts (*2*) a quantity that has been found to vary from face to face (*18–21*). The application of crystal-field theory to catalysis also predicts a variation of rate with crystal orientation (*4, 22, 23*). Such variations of activity with surface orientation have been demonstrated experimentally for reactions other than the N_2O decomposition by a number of investigators.

* This work was performed under the auspices of the U. S. Atomic Energy Commission.

Gwathmey and co-workers (*1*) found a variation of rate with orientation for metallic catalysts in the H_2, O_2 reaction and for the decomposition of CO. Similar results were found by others for the decomposition of formic acid by copper (*7*) and silver (*6*).

We have measured activation energies and pre-exponential factors for the N_2O decomposition on the {100}, {110}, and {111} faces of single-crystal CoO and the {100} face of single-crystal CoO-MgO solid solution. The catalysts were initially outgassed in an ultra-high vacuum at 450°C. Nitrous oxide pressures were around 45 to 90 torr; the reaction temperature range was 250–500°C. Catalyst surface areas were about 2–5 cm^2 and were determined from the crystal dimensions.

Experimental

Materials

1. N_2O was procured from a commercial supplier, nominally 98.0% pure. It was further purified by being passed slowly over a trap cooled in dry ice–Freon TA mixture and was then stored in a glass bulb. Mass spectrographic analysis after purification showed it to consist of >99.4% N_2O with 0.5% CO_2, ~0.01% O_2, and <0.1% H_2O.

2. A large cobalt oxide single crystal, 1 cm in diameter and 5 cm long was prepared from reagent grade Co_3O_4 by the Verneuil process with an arc-image furnace. From chemical analysis its formula was found to be $CoO_{1.03}$, while spectrographic analysis gave total cation impurity content of <0.5%—about the same as the Co_3O_4 powder from which it was made. Thin rectangular wafers having the {100}, {110}, and {111} orientations were cut from the large crystal. Because of finite thickness, about 25% of the total area of the {110} wafer had nonnominal orientation ({100} and {111} planes); while this percentage for {111} was 20%, consisting exclusively of {100} planes. Only {100} faces were exposed on the {100} wafers. The wafers were mechanically polished, and the disturbed layer was removed by chemically polishing a few seconds in hot H_3PO_4, followed by washing in water, acetone, and alcohol. The change from a "disturbed" to a smooth surface could be detected by electron diffraction. The spot and line diffraction pattern characteristic of a partly random arrangement was converted to a simple spot pattern by chemical polishing. X-Ray Laue patterns, electron diffraction patterns, and X-ray diffractometer tracings showed that the cut and polished faces were within one or two degrees of the nominal orientation. The diffraction patterns indicated the presence of Co_3O_4 on the surface. The chemical polishing, which was necessary to remove the disturbed layer, apparently uncovered "inclusions" of Co_3O_4, which appeared as projections on the surface, having the symmetry of the surface. They introduced nonnominal faces whose areas amounted to about 7% of the total area on the {111} crystal and were much less on the other samples. Only if they were especially active would these inclusions have contributed appreciably to the observed rate. Evidence that they were not very active was given by the observation (see below) that the {111} sample, containing the greatest concentration of inclusions, was not the most active (it behaved much like the {100}, which had the least inclusion concentration).

3. CoO-MgO single-crystal solid solutions were prepared from single-crystal MgO by interdiffusion, in which Co^{2+} replaced Mg^{2+} substitutionally (*24*). The crystals were mechanically polished, then chemically polished in H_3PO_4 and washed. Electron microscopic examination showed a very smooth surface. Laue patterns and chemical etching demonstrated that the CoO-MgO was a single crystal. The surface concentration of cobalt oxide was estimated from electron probe analysis to be 60 mole %.

Apparatus

Figure 1 shows a schematic diagram of the apparatus. The reaction chamber was made small so as to minimize the contribution of the homogeneous reaction (*25*, *26*) to the measured rate. It was surrounded by a nickel-plated copper can and a mag-

netically actuated, evacuated plug [Fig. 1(A)] to keep the reaction zone at constant temperature (within 1%). When the plug was moved to the left, the chamber was connected by wide-bore tubing to the ultra-high-vacuum system so that it could be speedily evacuated. The reactor was constructed so that samples could be moved into and out of the reaction zone, without opening the system to the atmosphere, with the help of a magnetically actuated carriage. Catalyst samples were removed and replaced in the reactor by a glass-blowing operation. For convenience, the reactor was loaded with several samples at one time.

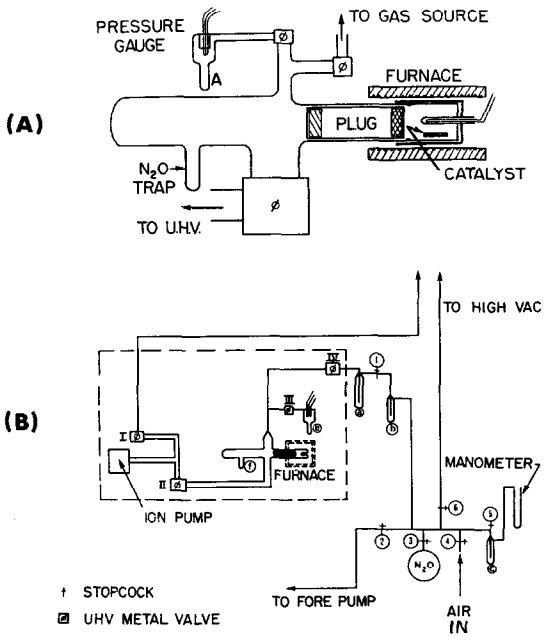

FIG. 1. (A) Schematic diagram of the reactor, made of quartz and Pyrex. The plug is shown in the position it has during reaction; the reaction volume is to its right. The plug and reaction volume are made of quartz. The reaction products are condensed at A; the N_2O trap is labeled (f) in (B). (B) Schematic diagram of apparatus. The numbers label valves, the letters label cold traps. The ultra-high-vacuum portion is enclosed within the dotted lines. The thermocouple pressure gauge is located at (e); it can be isolated from the rest of the system by closing valve III.

The product gas pressure was measured with a directly heated thermocouple gauge (*27*, *28*). It was calibrated against a McLeod gauge, with dry air, which was considered sufficiently close in chemical composition to the $2N_2 + O_2$ product gas for this purpose.

Procedure

After the reactor had been loaded with catalyst samples, the usual procedures of bake-out and pump-down to achieve $<10^{-9}$ torr were followed, the Vac-Ion pump current serving to indicate the pressure. The system was baked out only after it had been opened to the atmosphere; evacuation to $\sim 5 \times 10^{-9}$ torr at reaction temperature followed each run. N_2O was introduced by slowly flowing it through a trap cooled with a dry ice–Freon TA mixture and then condensing it in (f) [Fig. 1(B)] with liquid nitrogen. The N_2O pressure during reaction was calculated from a knowledge of the apparatus volumes and the pressure (measured with a mercury manometer) before expansion.

A run was started after temperature equilibrium had been established, and evacuation to $\sim 5 \times 10^{-9}$ torr accomplished. "Zero" time was established by rapidly evaporating the N_2O by gentle warming; the evaporation took place within 1 min. Reaction was allowed to proceed for the appropriate time, after which the N_2O was recondensed in (f). The N_2O and O_2 were transferred to (e) (Fig. 1) by condensation with liquid helium. The resulting pressure (P_e) was measured after Valve III was shut, and the trap warmed to room temperature. The reaction rate was calculated from P_e and the reaction time (see below). In order to measure the extent of reaction in the gas phase and the walls, the catalyst was removed from the reaction zone and a series of "blank" runs were made at various temperatures. The blank rates were subtracted from the total rates to obtain the net rate due to the catalyst alone. The reactant gas was replaced infrequently because each run consumed only a small fraction (see below) of the N_2O. Calculations and experimental measurement of the N_2O pressure remaining after a number of runs confirmed this.

Rate Calculations

In keeping with previously published findings for the N_2O decomposition by *p*-type catalysts (*9*, *12*) we assumed the reaction rate to be proportional to the N_2O pressure, and neglected the oxygen pressure dependence. In our experiments the reactant pressure was essentially constant during a run (only about 5×10^{-3} % of the N_2O reacted) and hence the oxygen pressure was always much lower than the N_2O pressure.

The "absolute rate constants," k_a (*29*) in units of cm/sec were calculated from the equation

$$k_a = \tfrac{2}{3} P_e V_e [P_N A t]^{-1} \qquad (1)$$

where P_e is the total product gas pressure measured in the volume V_e (Fig. 1), P_N is the N_2O pressure, A is the sample area, and t is the reaction time measured from the time of evaporation of the N_2O. Units are P_e and P_N, torr; V_e, cm^3; A, cm^2; t, sec. The volume V_e was 35 cm^3 in our apparatus.

The N_2O condensation time was occasionally, for active catalysts, an appreciable fraction of the total reaction time and had to be taken into account. This was done by assuming that the rate of condensation of N_2O was given by the equation for the pumping speed of a cold trap (*30*). The correction obtained was

$$t = t_0\{1 + [(1 - e^{-K\tau})/Kt_0]\}. \qquad (2)$$

Here, t is the corrected reaction time, τ is the condensation time, t_0 is the time from evaporation of N_2O to the start of condensation. The exponential term was always equal to 10^{-2} or less, while $[Kt_0]^{-1}$ was usually less than 0.02 and only rarely did it get as large as 0.08. Thus, even when the

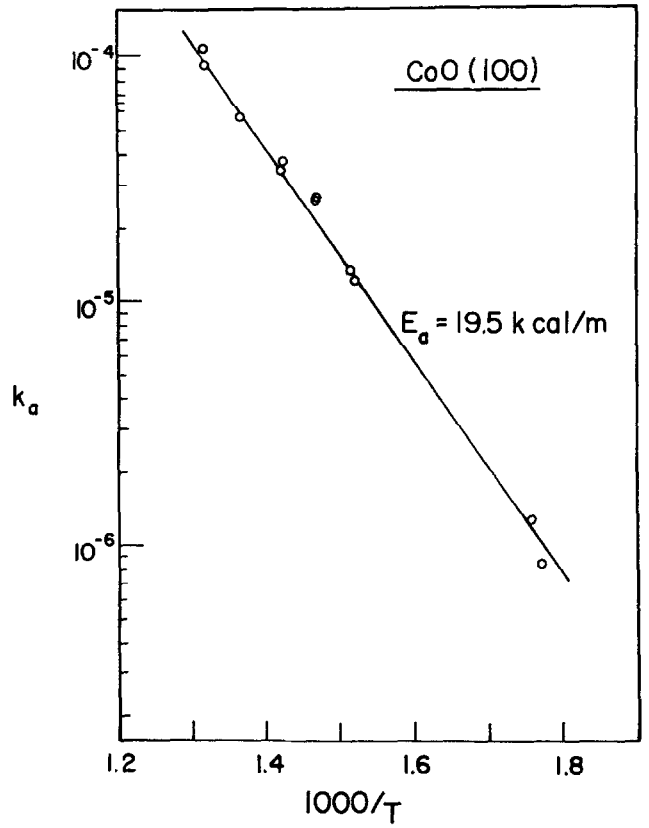

FIG. 2. Arrhenius plot for CoO {100}, random temperatures. Log k_a(cm/sec) is plotted vs. 1000/T(°K). Surface area, 3.79 cm^2; N_2O pressure 90.3 torr.

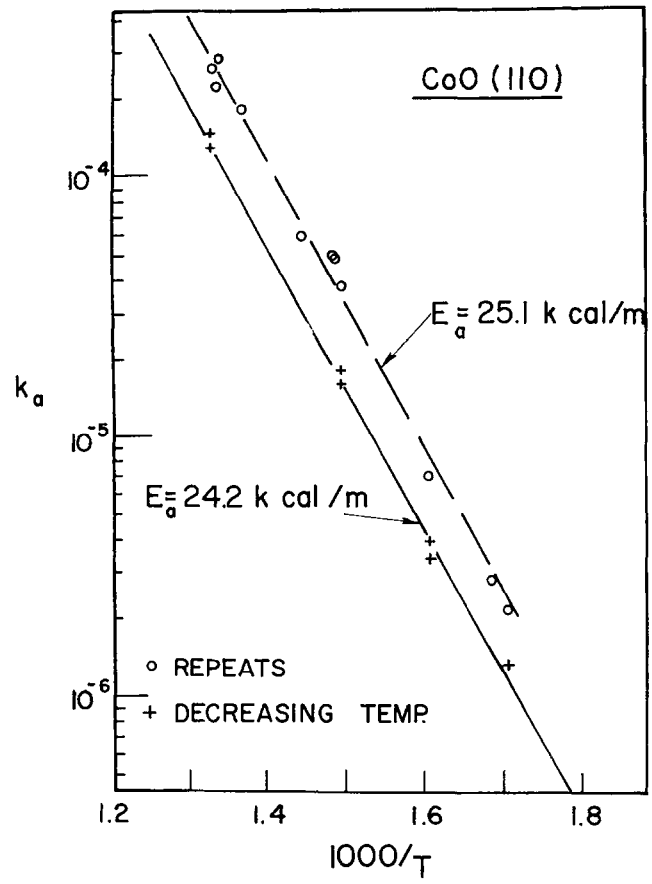

FIG. 3. Arrhenius plot for CoO {110}. Crosses mark decreasing temperature points; open circles mark random temperature points. Log k_a(cm/sec) is plotted vs. $1000/T$(°K). Surface area, 1.73 cm²; N_2O pressure 89.0 torr.

correction term was significant, it was always less than 10%.

RESULTS

CoO

The data for pure single-crystal cobalt oxide are displayed in Figs. 2, 3, and 4 as Arrhenius plots, and in table form in Table 1. The quantities plotted are absolute rate constants, k_a, in units of cm/sec. The blank rates, amounting to about 1%, have been subtracted from the total rates.

For each of the samples, "activation" was required, consisting of five runs made at the higher temperatures, about 480°C. This procedure increased the rates about 50-fold, after which, for the {100} crystal, no further change was noted (Fig. 2). The runs in this plot represent random choices of temperature. After activation for the {110} orientation, a good straight-line Arrhenius plot resulted for decreasing temperatures (Fig. 3, solid line). Upon raising the temperature to check points at 480°C, the rate was found to have increased substantially; cyclic variation of the temperature between high and low values produced the points designated by open circles in Fig. 3. The least-squares line for the latter points is given by the dotted line. For the {111} crystal (Fig. 4), the original run was also made with decreasing temperatures; a "repeat" run was made with random temperatures some weeks after. In this case, both the activation energies and pre-exponential

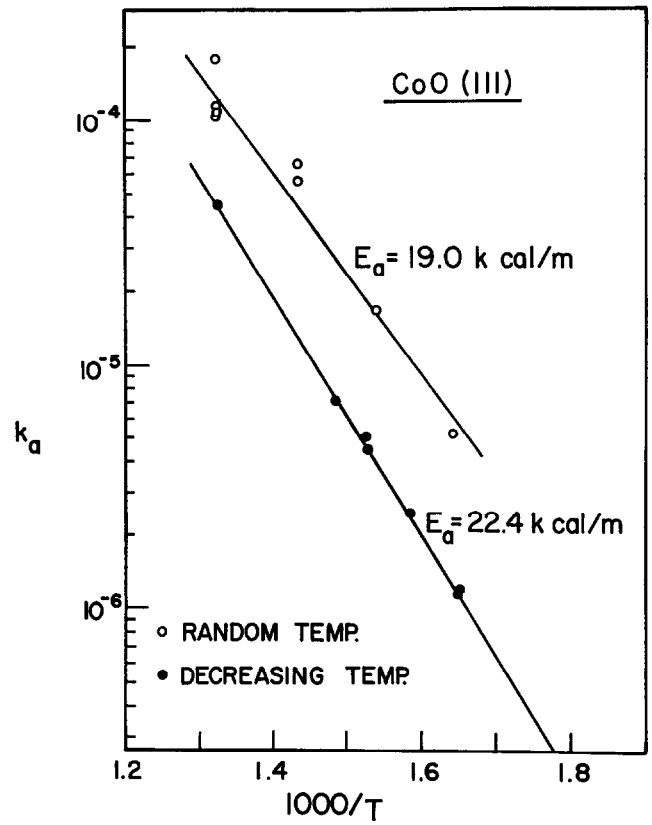

FIG. 4. Arrhenius plot for CoO {111}. Solid points are for decreasing temperatures, open circles mark random temperature points: Log k_a(cm/sec) is plotted vs. $1000/T$(°K). Surface area, 2.60 cm². N_2O pressures, solid points, 90.3 torr; open points, 89.0 torr.

terms were different. Calculated activation energies and preexponential terms for both random and continuously decreasing temperatures are listed in Table 1.

CoO-MgO

Figure 5 gives Arrhenius plots made with random selection of temperature for CoO-MgO that had been mechanically

TABLE 1

DATA SUMMARY FOR N_2O CATALYSIS BY PURE CoO AND BY CoO-MgO

Catalyst	Area (cm²)	P_{N_2O} (torr)	E_a(kcal/mole)[a]	Pre-exp. (cm sec^{-1})[a]
CoO {100}	3.79	90.3	19.5 ± 0.1 (R)	62 ± 2% (R)
CoO {110}	1.73	89.0	24.2 ± 0.1 (D)	370 ± 6% (D)
	1.73	89.0	25.1 ± 0.8 (R)	1365 ± 100% (R)
CoO {111}	2.60	90.3	22.4 ± 0.1 (D)	46 ± 2% (D)
	2.60	89.0	19.0 ± 0.1 (R)	13 ± 30% (R)
CoO-MgO {100}[b]	3.15 3.15	88.5 45.5	26.5 ± 0.2 (R)	117 ± 13% (R)
CoO-MgO {100}[c]	4.80	89.6	39 ± 4.7 (R)	3.6×10^4 ± 100% (R)
MgO [ref. (9)]	—	760	35	—

[a] (R), Random temperatures; (D), decreasing temperatures.
[b] Mechanical polish.
[c] Chemical polish.

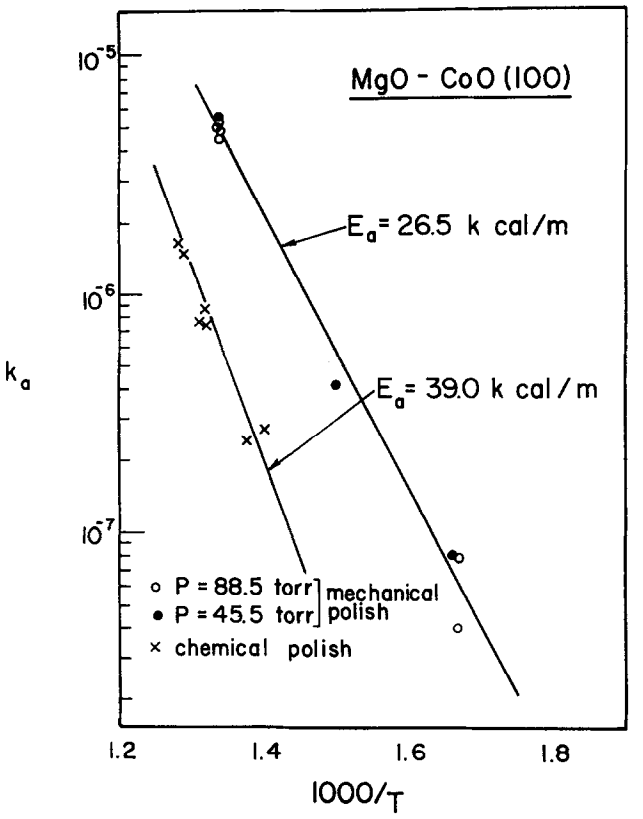

FIG. 5. Arrhenius plot for CoO-MgO {100}. Crosses are for chemically polished sample, round points are for mechanically polished sample. Log k_a(cm/sec) is plotted vs. $1000/T$(°K) for random choice of temperatures. Surface area, 4.8 cm² (chemical polish) and 3.15 cm² (mechanical polish). N_2O pressure chemical polish, 89.6 torr; mechanical polish, 88.5 torr.

polished only, and for CoO-MgO with which the mechanical polish was followed by a chemical polish in H_3PO_4. With these samples the blank rates were about 20% of the total rate; the data presented here were calculated from the net rates for CoO-MgO catalysis. In Fig. 5, the solid points were made at 45.5 torr, while the open points were at 88.5 torr. The fact that they all lie on a straight line is good evidence that the reaction is first order in N_2O pressure.

Table 1 compares the activation energies and pre-exponential factors for the CoO-MgO runs with those for CoO and MgO [the latter from the data of Matsuura *et al.* (*9*)]. The data show that the mechanically polished solid solution acts like pure CoO while the chemically polished crystal acts like MgO.

DISCUSSION

The effect that crystal surface structure would be expected to have upon activation energy can be quantitatively estimated by use of crystal-field theory (*4*, *22*). The calculations follow very closely those made by Haber and Stone (*22*) for oxygen adsorption on NiO. If it is assumed that the rate-determining step is the desorption of oxygen from perfect CoO surfaces, then these calculations show that the {110} orientation would be expected to have an activation energy which is 6.9 kcal/mole higher than the {100} orientation and 3.5 kcal/mole higher than the {111} face.

Our experimentally observed activation energy for the {110} crystal was, in fact, higher than either the {100} or {111} activation energies. However, their magnitudes depended upon the way that the temperature was varied in constructing the Arrhenius plots. As can be seen from Table 1, based on random choice of temperatures, the activation energy for the {110} crystal was about 6 kcal/mole greater than either of the others. If steadily decreasing temperatures were used for the {111} and {110}, the {110} — {100} activation energy difference would be 5 kcal/mole, while the {110} — {111} difference would be about 2 kcal/mole. This quantitative uncertainty was mostly due to the large effect that catalyst pretreatment had upon the {111} activation energy. This, along with the activation phenomenon and the pre-exponential variation exhibited by the {110} (see Fig. 3 and Table 1), indicates that pretreatment may have been so important that an unequivocal interpretation of observed activation energy differences in terms of surface geometry can not be made.

The mechanisms by which pretreatment influenced the catalyst activities are still obscure. It is conceivable that structural rearrangement could be involved. Low-temperature structural rearrangements (facet formation) during catalysis have been observed with metal crystals (*1*); epitaxial oxide growths to form low-energy metal–oxide interfaces apear to be essential in these cases. This mechanism may be operable for CoO, faceting being stimulated by surface Co_3O_4 layers. Formation of Co_3O_4 from CoO during N_2O catalysis has been previously reported by Matsuura *et al.* (*9*). The results of these investigators also provided evidence that this type of oxidation without facet formation could not account for our observation of an increase in activity, since they found that the production of Co_3O_4 formed a less active catalyst.

Another likely cause would be nonequilibrium adsorption of oxygen and possibly impurities. It would seem that the adsorption–desorption reactions of oxygen that are known to occur on the *p*-type semiconductors (*9, 12, 22, 23*) (which involve both labile and tightly held oxygen, and incorporation of oxygen into the lattice) could provide an explanation. It should be recognized too, that if oxygen adsorption were important, the rate of diffusion of oxygen from our reaction zone via the plug might become an important factor in causing pretreatment of the sample to affect its activity. More research will be needed to completely understand these phenomena.

The CoO-MgO {100} catalysts (60% cobalt, 40% magnesium) were much less active *per cobalt atom* than the pure CoO catalysts. They also exhibited a much higher activation energy than the CoO {100} and showed a distinct relationship between crystal preparation and activation energy (Fig. 5). One would expect CoO and NiO to behave similarly, yet Cimino *et al.* (*31*) found that powdered MgO containing less than 10 atom % of nickel gave a lower activation energy than pure NiO, and they attributed this difference to weaker bonding of oxygen by isolated Ni^{2+}. We find the opposite to be the case with CoO-MgO, dilution of Co aparently increasing the oxygen bond strength. Our observation of two activation energies for the mixed crystals, one similar to that found for MgO (*9, 31*), may be due to preferential solution of Co by H_3PO_4. If so, it emphasizes the importance of having the transition metal ions present in the adsorbing surface. This is support for a localized bond theory for chemisorption and catalysis such as crystal-field theory rather than a boundary-layer theory.

Acknowledgments

The authors gratefully acknowledge the help of Dr. Paul Stablein in furnishing the cobalt oxide crystals, and of Dr. Raymond Hart and his group in assisting with the electron microscopic and diffraction studies on the crystals. Their sincere thanks are also due to their colleague, Dr. Dennis W. Readey for stimulating discussions.

References

1. Gwathmey, A. T., and Cunningham, R. E., *Advan. Catalysis* **10**, 57 (1958).
2. Vol'kenshtein, F. F., "Electronic Theory of Catalysis on Semiconductors" (English

Transl. by M. G. Anderson), Pergamon Press, New York, 1963.
3. PARRAVANO, G., *Gazz. Chim. Ital.* **91**, 467 (1961).
4. DOWDEN, D. A., AND WELLS, D., *Actes Congr. Intern. Catalyse, 2e, Paris, 1960* **2**, 1499 (1961).
5. BAGG, J., JAEGER, H., AND SANDERS, J. V., *J. Catalysis* **2**, 449 (1963).
6. SOSNOVSKY, H. M. C., *J. Chem. Phys.* **23**, 1486 (1955); *J. Phys. Chem. Solids* **10**, 304 (1959).
7. RIENÄCHER, G., AND VÖLTER, J., *Z. Anorg. Allgem. Chem.* **302**, 292, 299 (1959).
8. HALL, J. W., AND RASE, H., *Ind. Eng. Chem.* **3**, 158 (1964).
9. MATSUURA, I., KABAKOWA, Y., AND TOYAMA, O., *Nippon Kagaku Zasshi* **81**, 1205 (1960).
10. AMPHLETT, C. B., *Trans. Faraday Soc.* **50**, 273 (1954).
11. STONE, F. S., RUDHAM, R., AND GALE, R. L., *Z. Elecktrochem.* **63**, 129 (1959).
12. WINTER, E. R. S., *Discussions Faraday Soc.* **28**, 183 (1959).
13. SCHWAB, G.-M., *et al., Z. Physik. Chem.* **B-9**, 265 (1930); **21**, 65 (1933); **25**, 411, 418 (1934).
14. SCHMID, G., AND KELLER, N., *Naturwiss.* **37**, 43 (1950).
15. HAUFFE, K., *in* "Semiconductor Surface Physics" (R. H. Kingston, ed.), p. 259 ff. Univ. of Pennsylvania Press, Philadelphia, Pennsylvania, 1956.
16. SCHWAB, G.-M., *in* "Semiconductor Surface Physics" (R. H. Kingston, ed.), p. 283 ff. Univ. of Pennsylvania Press, Philadelphia, Pennsylvania, 1956.
17. RHEAUME, L., AND PARRAVANO, G., *J. Phys. Chem.* **63**, 264 (1958).
18. MITROFANOV, O. V., *Soviet Phys.—Cryst. (English Transl.)* **8**, 169 (1963).
19. ALLEN, F. G., AND FOWLER, A. B., *J. Phys. Chem. Solids* **3**, 107 (1957).
20. ALLEN, F. G., AND GOBELLI, G. W., *J. Appl. Phys.* **35**, 597 (1964).
21. DILLON, J. A., JR., AND FARNSWORTH, H. E., *J. Appl. Phys.* **29**, 1195 (1958).
22. HABER, J., AND STONE, F. S., *Trans. Faraday Soc.* **59**, 192 (1963).
23. CHARMAN, H. B., DELL, R. M., AND TEALE, S. S., *Trans. Faraday Soc.* **59**, 453 (1963).
24. ZAPLATYNSKY, I., J. *Am. Ceram. Soc.* **45**, 28 (1962).
25. HINSHELWOOD, C. N., AND BURK, R. E., *Proc. Roy. Soc. (London)* **A106**, 284 (1924).
26. JOHNSTON, H. S., *J. Chem. Phys.* **19**, 663 (1951).
27. BENSON, J. M., *Trans. Vacuum Symp. 1956, Chicago, Illinois*, p. 87.
28. BUNKER, W. M., *Proc. Instr. Soc. Am. 1954*, Paper 54-43-2.
29. LAIDLER, K. J., *in* "Catalysis" (P. H. Emmett, ed.), Vol. 1, p. 119. Reinhold, New York, 1954.
30. LOEVINGER, R., *in* "Vacuum Equipment and Techniques" (A. Guthrie and R. K. Wakerling, eds.), p. 51. McGraw-Hill, New York, 1949.
31. CIMINO, A., *et al., J. Catalysis* **5**, 271 (1966).